Tailoring of internal fields in AlGaN/GaN and InGaN/GaN heterostructure devices

J. L. Sánchez-Rojas, J. A. Garrido, and E. Muñoz
Departamento de Ingeniería Electrónica, E.T.S. Telecomunicación, Universidad Politécnica de Madrid, Ciudad Universitaria, 28040 Madrid, Spain
(Received 23 June 1999)

A study of the internal electric field distributions in $Al_xGa_{1-x}N$/GaN and $In_xGa_{1-x}N$/GaN heterostructures grown on (0001) GaN is presented. The fields are deduced taking into account the device structure, background doping, and the difference in the total (spontaneous and piezoelectric) polarization of the layers. Two basic structures, a multiple quantum well in the depletion region of a *p-n* junction and the heterojunction field effect transistor, are analyzed. The cases where the field distribution can be approximated analytically are discussed. When charge accumulation is present at the interfaces, a self-consistent solution of the Schrödinger and Poisson equations is obtained. By comparing with available experimental data, the polarization field in $Al_xGa_{1-x}N$/GaN heterostructures has been estimated for two Al contents.

I. INTRODUCTION

The optical and electronic properties of GaN and related semiconductors make them suitable for a variety of device applications, such as light emitting diodes and lasers for a wide spectral range,[1] and high-power heterostructure transistors (HFET's).[2] Despite the significant progress in material fabrication and in the development of these structures, a number of fundamental aspects of GaN-based heterostructures are not yet well understood. In particular, polarization fields of considerable magnitude are present, inducing high-sheet carrier concentrations in the case of HFET devices,[3,4] and being also responsible for unique optoelectronic properties in the case of quantum well (QW) based structures.[5–8] The origin of these polarization fields is the symmetry of the GaN wurtzite structure, and it has been shown that both piezoelectric (strain-induced) and spontaneous (zero strain) polarizations have significant and comparable magnitudes in III-N heterostructures.[9]

This paper is focused on how these polarization fields lead to electric fields that modify the device bandstructure, and on presenting design expressions to tailor the electric fields present in heterostructure devices. Such information is needed to determine the resulting potential profile in the heterostructure, as it is required for the proper interpretation of optoelectronic experimental data in quantum wells. These are, for example, the cases when optical transitions in a QW are analyzed to study the intrinsic quantum confined Stark effect,[8] or when the field in the QW is partially screened by the photoexcited electrons and holes,[6] or the situation when the QW transition energies are modified by applying an external bias.[5] In a simple approach, the field in the well is calculated from the polarization of the layers neglecting the device geometry and the boundary conditions imposed by the device configuration.[10] These variables determine the relative position of the Fermi level with respect to the conduction band at different points of the structure. In other calculations, the device geometry is taken into account by assuming a periodic boundary condition equivalent to taking a total potential drop in one period (well and barrier) equal to zero.[8,11,12] This same approach was considered in the early studies on $In_xGa_{1-x}As$/GaAs piezoelectric quantum wells.[13,14] Subsequent experimental results obtained in [111]-oriented $In_xGa_{1-x}As$/GaAs structures led to a more general description of the electric fields being present in piezoelectric MQW structures.[15] From that experience, in this paper, we present a general analysis of the electrostatic fields in GaN-based heterostructures, and, when possible, accurate analytical expressions for these fields are presented. These expressions aim to help in the design process of III-N heterostructures where electric fields are to be tailored.

II. UNDOPED III-N HETEROSTRUCTURES

Three basic heterostructures are considered to illustrate the most simple approximations. Let us first consider a single $Al_xGa_{1-x}N$ layer embedded into a thick GaN layer with the [0001] orientation. We neglect the residual strain in the two GaN cladding layers (they are thick enough to have relaxed the strain due to the lattice mismatch with the substrate). The lattice constant of $Al_xGa_{1-x}N$ is smaller than that of GaN, but for a sufficiently thin $Al_xGa_{1-x}N$ layer, the lattice constant mismatch is accommodated by internal strain rather than by the formation of dislocations. The biaxial tension in $Al_xGa_{1-x}N$ is given by the three nonzero components of the strain tensor

$$\varepsilon_1=\varepsilon_2=\frac{a_c-a_e}{a_e}, \tag{1}$$

and

$$\varepsilon_3=-\frac{2c_{13}}{c_{33}}\frac{a_c-a_e}{a_e}, \tag{2}$$

where c_{ij} are the elastic constants, and a_c and a_e are the in-plane lattice constants of the cladding layer (GaN in our example) and the epilayer ($Al_xGa_{1-x}N$), respectively. The strain induces a piezoelectric polarization of the epilayer in the growth direction, that can be calculated either using the e_{ij} or the d_{ij} piezoelectric coefficients as

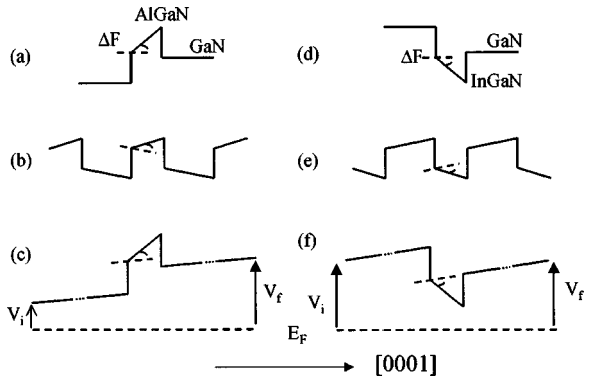

FIG. 1. Conduction-band profiles for: $Al_xGa_{1-x}N$ with semi-infinite GaN cladding layers (a). Al_xGa_{1-x}/GaN periodic structure (b). $Al_xGa_{1-x}N$ with finite GaN claddings (c). $In_xGa_{1-x}N$ QW with semi-infinite GaN barriers (d). $In_xGa_{1-x}N$/GaN periodic MQW (e), and $In_xGa_{1-x}N$ QW with finite barriers (f). ΔF is defined in the text as the change in the slope of the potential at the interface.

$$P_p = 2\left(e_{31} - \frac{c_{13}}{c_{33}} e_{33}\right)\varepsilon_1 \quad \text{or} \quad P_p = 2d_{31}\left(c_{11} + c_{12} - \frac{2c_{13}^2}{c_{33}}\right)\varepsilon_1 . \tag{3}$$

Besides, a spontaneous polarization in both the cladding and the epilayer must also be considered. This symmetry-related polarization has been calculated for GaN, AlN and InN by Bernardini.[9] For $Al_xGa_{1-x}N$ and $In_xGa_{1-x}N$ we assume that the spontaneous polarization can be estimated using a linear interpolation of the values for the binary compounds. Once the total polarization of the layers is known, we have to apply a boundary condition at the interface of two layers (say 1 and 2), requiring the conservation of the macroscopic displacement field in the growth direction:

$$\kappa_1 F_1 + P_1 = \kappa_2 F_2 + P_2 ; \tag{4}$$

where κ_i is the dielectric constant, and P_i and F_i are the total polarization and electric field in layer ''*i*.'' From expression (4), we can obtain the discontinuity in the electric field at the interface of the two layers. The approximation of $\kappa_1 \approx \kappa_2$ is made in order to have a simple expression for this field discontinuity

$$\Delta F = F_2 - F_1 = \frac{P_1 - P_2}{\kappa} . \tag{5}$$

To determine the electric field distribution in the structure, additional information about the doping and thickness of the layers is required. The simplest approximation assumes undoped semi-infinite cladding layers, where there is zero-electric field. In this case, Eq. (5) tells us directly the field in the epilayer. The schematic bandstructure is shown in Fig. 1(a) for this simple $Al_xGa_{1-x}N$/GaN double heterojunction.

This basic structure is of little practical interest, since the active region of usual QW-based devices is only a few hundred angstroms, and electrostatic fields may be significant in those cladding layers and cannot be neglected. As a second example, let us now consider a periodic $Al_xGa_{1-x}N$/GaN MQW structure. A pseudomorphic sequence of layers with the in-plane lattice constant given by that of a thick, relaxed GaN buffer is assumed in this case and throughout the paper. Very often, an electric field distribution is assumed such that the conduction-band profile is also periodic,[8,11] and hence the potential drop across two consecutive layers, of thicknesses L_1 and L_2, is:

$$F_1 L_1 + F_2 L_2 = 0, \tag{6}$$

giving

$$F_2 = \frac{L_1(P_1 - P_2)}{(L_1 + L_2)\kappa} \quad \text{and} \quad F_1 = \frac{L_2(P_2 - P_1)}{(L_1 + L_2)\kappa} . \tag{7}$$

The resulting conduction-band profile in this MQW structure is shown in Fig. 1(b). Expressions (6) and (7) have been used to estimate the fields in multiple quantum well structures that are clearly not periodic.[8]

Let us now consider the case of undoped GaN/$Al_xGa_{1-x}N$/GaN double heterojunction with arbitrary dimensions. We call V_f to the difference between the conduction band minimum and the Fermi level at one end of the structure and V_i to the same difference at the end of the structure close to the substrate. Assuming that the Fermi level is constant throughout the layers and calling V_{fi} to the difference between the above values, i.e., the difference in the energies of the conduction-band minima at both ends of the structure, we have

$$F_1(L_1 + L_3) + (\Delta F + F_1)L_2 = V_{fi} , \tag{8}$$

where L_1, L_2, and L_3 are the respective thicknesses of the GaN/$Al_xGa_{1-x}N$/GaN layers. This case is plotted in Fig. 1(c). Neglecting the background doping and assuming that the Fermi level is around the middle of the gap at both ends, surface and substrate side, we have $V_{fi} = 0$, and therefore,

$$F_1 = \frac{L_2(P_2 - P_1)}{(L_1 + L_2 + L_3)\kappa} \quad \text{and} \quad F_2 = F_1 + \Delta F. \tag{9}$$

These three simple situations analyzed above can also be considered when the $Al_xGa_{1-x}N$ strained layer is replaced by $In_xGa_{1-x}N$. In this case, the $In_xGa_{1-x}N$ lattice constant is larger than that of GaN and the strain corresponds to biaxial compression. The sign of ΔF changes and the conduction band profile for the semi-infinite GaN claddings, for the periodic potential approximation and for the finite device are shown in Figs. 1(d), 1(e), and 1(f), respectively.

III. DOPING EFFECTS AND *P-N* JUNCTION STRUCTURES

A. Role of polarization fields in *p-n* junctions

Let us now consider a pseudomorphic *n*-type doped MQW with strained $Al_xGa_{1-x}N$ barriers (thickness L_{bi}) and GaN quantum wells (thickness L_{wi}), incorporated in the *n* region of a *p-n* junction diode. Let us assume a thick (enough to accommodate the depletion region) *p*-type-doped GaN layer on the top. For simplicity, we assume that both the donor and acceptor concentrations, N_D and N_A, are uniform in the *n* and *p* region, respectively, although results can easily be generalized. The schematic conduction-band profile is shown in Fig. 2(a). For the calculation of the fields we use two well-known approximations.[16] One is the abrupt metallurgical junction hypothesis, and the other one is the depletion approximation, where a depleted region with negative

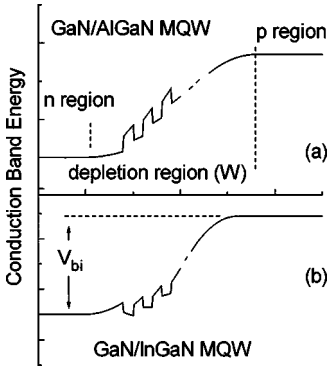

FIG. 2. Sketch of the potential variation with distance in a GaN p-n junction with $Al_xGa_{1-x}N$/GaN (a), or $In_xGa_{1-x}N$/GaN (b), MQW in the n region.

charge is in a region of length X_p in the p side and a depleted region with positive charge is in a region of length X_n in the n side. The charge distribution must include the polarization charges associated with polarization fields (piezoelectric +spontaneous) at the interfaces.

We now apply the charge neutrality condition,

$$N_A X_p = N_D X_n \tag{10}$$

and the superposition principle to find the total potential drop in the device, that, in the absence of an externally applied bias, is precisely the built-in voltage V_{bi}. This voltage can be computed from the GaN band-gap energy and from the doping level in the n- and p-type regions.[16] The total potential drop is the sum of that due to the doping and that due to the field discontinuities produced by the polarization fields, resulting a total depletion width of

$$W = X_n + X_p = \sqrt{\frac{2\kappa}{q}\left(\frac{N_A + N_D}{N_D N_A}\right)\left(V_{bi} - \sum_i \Delta F_i L_{bi}\right)}. \tag{11}$$

The strength of the electrostatic field changes linearly with distance from the junction, x

$$F(x) = F_m - \frac{qN_d}{\kappa}x, \tag{12}$$

in the n-type region, and

$$F(x) = F_m - \frac{qN_A}{\kappa}x \tag{13}$$

in the p-type region. F_m is the maximum field in the junction, and is given by the equation for the total potential drop

$$V_{bi} = \sum_i \Delta F_i L_{bi} + \frac{1}{2}F_m W. \tag{14}$$

In Eqs. (11) and (14) each term of the form $\Delta F_i L_{bi}$ corresponds to the potential drop in each of the $Al_xGa_{1-x}N$ barriers, and they are positive, according to the values of the polarization fields. This means that both the maximum electrostatic field and the depletion width are lower than the values calculated neglecting the effect of polarization charges. The magnitudes of the built-in voltage and the polarization-related potential drop [sum under the square root in Eq. (11)] may be comparable and give a negative value under the square root. There is, however, a limit to our depletion approximation, given by the fact that electrons can accumulate at the GaN/$Al_xGa_{1-x}N$ interface closest to the substrate side of the structure, forming a two-dimensional channel confined by the $Al_xGa_{1-x}N$-GaN band discontinuity.

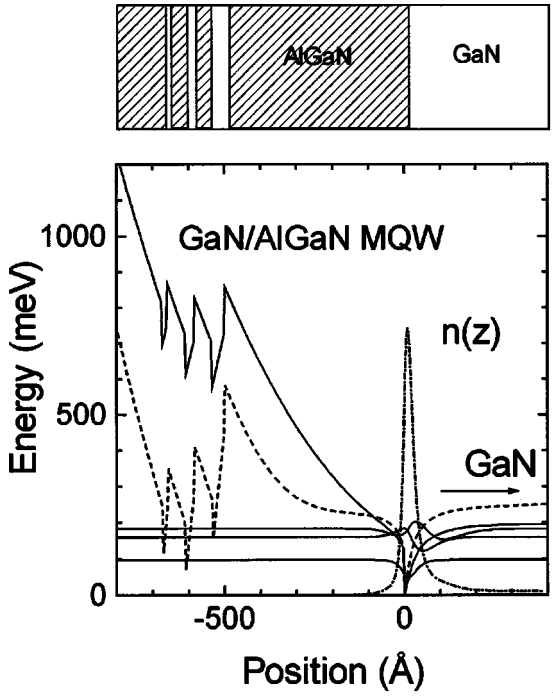

FIG. 3. Energy-band diagram for three GaN/$Al_xGa_{1-x}N$ QW's of 5, 9, and 13 monolayers. The sequence of layers is shown in the upper part of the figure. The potential calculated using the theoretical polarizations is plotted with dashed line and that produced by the fitting to the experimental field in the wells (after Ref. 8) is in solid line. The first three wavefunctions are superimposed upon their respective energy levels. The self-consistent charge distribution is shown with dot-dashed line.

If we now consider a dual structure, composed of [0001]-oriented $In_xGa_{1-x}N$/GaN QW's, the field discontinuities have opposite sign and there is an increase in the depletion width and in the maximum field strength present in the junction. Figure 2(b) displays the conduction-band profile in this case, sketched using the depletion approximation. In general, the fields might be different from well to well, depending on the density of ionized impurities as given by expression (12).

B. Charge accumulation effects

We now consider an example of III-N heterostructure where carrier accumulation is expected to be present, and a self-consistent calculation of the fields has to be performed. The structure has been fabricated to study the influence of built-in polarization fields on the quantum confined Stark effect.[8] It consists of a relaxed GaN buffer layer, 500 Å of $Al_{0.11}Ga_{0.89}N$, three GaN quantum wells of widths 13, 9, and 5 monolayers separated by 50 Å $Al_{0.11}Ga_{0.89}N$ barriers, and 300 Å-thick $Al_{0.11}Ga_{0.89}N$ on the top (Fig. 3). The sample was nominally undoped, but n-type background doping of around $10^{17}\,cm^{-3}$ can be expected in the molecular-beam

epitaxy (MBE) growth. Comparing this sample with the p-n junction structure analyzed above, we have to take into account that an $Al_xGa_{1-x}N$ terminated structure should have a surface voltage due to the pinning of the Fermi level somewhere in the middle of the gap. Therefore, this is a particular case of our model in which there is not a p-type region, but the built-in voltage is given by the pinning of the Fermi level. The situation is similar to the one-side abrupt p^+-n junction.

For the $Al_{0.11}Ga_{0.89}N/GaN$ heterojunction, using the values for the polarization fields taken from Ref. 9, $\Delta F = 1.1\,\mathrm{MV/cm}$ is obtained. The total barrier length of the structure is $500\,\text{Å} + 2\times 50\,\text{Å} + 300\,\text{Å} = 900\,\text{Å}$ (the barrier close to the substrate, the two barriers for the quantum well in the middle, and the barrier on top of the structure are added). Therefore, the total potential drop associated with polarization fields is calculated as 9.9 volts. This is much higher than any reasonable value for the built-in voltage in the structure. This is clear example where carrier accumulation must occur at the bottom $GaN/Al_{0.11}Ga_{0.89}N$ interface, and the fields have to be deduced from a self-consistent calculation including the background doping and the surface voltage. We have performed this type of calculation following the scheme previously described for piezoelectric $In_xGa_{1-x}As/GaAs$ structures.[17] The material parameters for the III-N system,[9] an electron effective mass of $0.22m_0$ and a conduction-band discontinuity given by 75% of the difference in $Al_xGa_{1-x}N$ and GaN band gaps have been used. We have incorporated the spontaneous polarization in all the layers along with the boundary conditions given by expression (5). The background doping can be determined from electrical measurements on single GaN layers grown separately under the same conditions. Typically, a donor concentration of around $10^{17}\,\mathrm{cm}^{-3}$ is found. The surface voltage is determined by the surface Fermi level pinning. The exact position of the Fermi level at the $Al_xGa_{1-x}N$ surface is not known. In order to explore the consequences of our model, we have assumed that the Fermi level on bare $Al_xGa_{1-x}N$ surface is at midgap, as in the well-established case of $Al_xGa_{1-x}As$.[18] The sensitivity of our result to this assumption is shown at the end of this section.

Figure 3 shows the results of the self-consistent calculation. First, we have considered exactly the same parameters, including the total field discontinuity of 1.1 MV/cm obtained from expression (5), as in Ref. 8. The field in the well calculated using the approximation of periodic potential, depends on the well width, as shown in expression (7), and is in the range of 750 to 620 KV/cm. The self-consistent potential profile shown in Fig. 3 (dashed line) allows us to deduce more accurately the field in each well, yielding values in the range of 850 to 900 KV/cm. This value is about twice the experimental field strength of 450 KV/cm estimated from a detailed analysis of the QW transition energies dependence on well width, as measured by photoluminescence.[8]

To track this problem, we performed a second calculation where the total field discontinuity is now varied, trying to get an agreement between the measured and the calculated fields in the well. The total field discontinuity has to be reduced from 1.1 MV/cm down to 650 KV/cm. It is worth noting that this field discontinuity is given by the difference in the total polarizations of the GaN and $Al_xGa_{1-x}N$ and hence we cannot split from this analysis, into values for the spontaneous polarization or for the piezoelectric polarization, separately. To obtain the best fit to the experimental electric field, the new conduction-band potential profile in the MQW is displayed in Fig. 3 as a solid line. As mentioned previously, there is charge accumulation at the $GaN/Al_xGa_{1-x}N$ interface close to the substrate. This figure also includes a plot of the first three confined electron wavefunctions and the charge distribution, $n(z)$, in the MQW structure. The calculated accumulated 2-D charge is $3\cdot 10^{12}\,\mathrm{cm}^{-2}$.

The same calculation procedure has been applied to a similar MQW structure now with four $GaN/Al_{0.11}Ga_{0.89}N$ quantum wells of different thicknesses (sample B in Ref. 8). We have found the same result for the field discontinuity at the $GaN\text{-}Al_{0.11}Ga_{0.89}N$ interface. In both cases, we have consistently assumed a surface Fermi level pinning at the middle of the band gap (a surface voltage of 1.8 V) and a background doping of $10^{17}\,\mathrm{cm}^{-3}$ donors. Since there is charge accumulation in both this and the previous structure, expression (11) and the related analytical formulas for the fields cannot be applied. However, an alternative analytical approximation to the field in the wells is now derived that can be used to study the effects of varying the structure critical parameters, as background doping, surface voltage or polarization fields.

Let us call V_{fi} the total potential drop in the region from the surface to the $GaN\text{-}Al_{0.11}Ga_{0.89}N$ interface at the substrate side. This voltage is given by the surface voltage (difference between the conduction band and the Fermi level at the surface) minus the difference between conduction band and Fermi level at that interface. This last term is much lower than the first one for Al contents lower than about 15% and 2-D charge densities higher than about $10^{12}\,\mathrm{cm}^{-2}$, as it is our case. The total potential drop is the sum of three terms due to the polarization fields, the background doping, and the accumulated charge at the interface.

$$V_{fi} = \sum_i \Delta F_i L_{bi} + \frac{qN_dW^2}{2\kappa} + F_sW, \tag{15}$$

where in the first term of the right-hand side the parameters are those used in Eq. (11), in the second term N_d is the residual doping, and W is the total separation between the surface and the 2-D accumulated charge. In the third term, F_s is the field due to the electrons at the interface. The above expression allows us to obtain an analytical estimation of the field in the well at a distance L_b from the substrate, i.e., the first QW grown. This is the sum of F_s and the field due to the ionized donors:

$$F_w = -\frac{qN_d}{\kappa}L_b + \frac{-V_{fi} + \sum_i \Delta F_i L_{bi} + \dfrac{qN_dW^2}{2\kappa}}{W}. \tag{16}$$

It is important to note that in the samples studied by Leroux *et al.*,[8] the values of the field in the well obtained by both the self-consistent calculation and by using expression (16), agree with the experimental value of 450 KV/cm. The magnitude of V_{fi} has been taken as 1.5 V (lower than the surface voltage of 1.8 V due to the contribution of the Fermi

level above the GaN conduction band at the interface with $Al_{0.11}Ga_{0.89}N$). The field discontinuity introduced by the polarization fields is the value that we have deduced above (650 KV/cm instead of the theoretical value of 1.1 MV/cm for GaN-$Al_{0.11}Ga_{0.89}N$), and the residual doping is the same in both MQW samples, $10^{17}\,cm^{-3}$ donors.

Expression (16) allows us to determine how a given error in the surface voltage leads to a corresponding error in the field discontinuity, ΔF, when the rest of the variables are kept constant. If the surface voltage is, for example, 1 V higher than the 1.8 V assumed, then our estimated field discontinuity of 650 KV/cm increases 1 V/900 Å or 111 KV/cm. The hypothesis of a pinning of the Fermi level at midgap is supported by a predicted reduction of the field discontinuity, with respect to the available theories, which is consistent with similar findings in several structures based on $Al_xGa_{1-x}N$/GaN for various Al contents. One of these cases is shown in the next section and additional compositions are considered in Ref. 4.

From the discussion in this section we conclude that the relative magnitudes of the built-in voltage and polarization-related potential drop in the whole structure determines whether or not there is charge accumulation. If there is such effect, expression (16) may give a good approximation to the exact self-consistent field determination.

IV. HETEROJUNCTION FIELD EFFECT TRANSISTORS

Let us note that the potential distributions plotted in Fig. 3 are very similar to those present in conventional $Al_xGa_{1-x}N$/GaN heterojunction field effect transistors.[2] In fact, we have used our model to simulate the electrical characteristics of this kind of structures, and by fitting the HFET experimental data, values of the polarization fields also lower than those calculated by Bernardini[9] have been obtained. Let us consider a HFET structure with a nonintentionally doped (NID) GaN channel-buffer layer, followed by a 30 Å-thick $Al_{0.22}Ga_{0.78}N$ spacer and an *n*-type-doped, 280 Å-thick, $Al_{0.22}Ga_{0.78}N$ barrier layer with a doping level of $2\times10^{18}\,cm^{-3}$. This structure has been experimentally studied in detail, and the results of the electrical and structural characterization will be reported elsewhere.[4] In this paper, we are interested, first, in the analogies with the structures described previously, justifying the self-consistent calculations, and second, in determining the polarization fields that are needed to fit the experimental HFET characterization results.

Our one-dimensional model for the heterojunction FET considers a Schottky barrier metal-semiconductor junction on top of the structure (gate), and applies the charge neutrality condition for the whole device (a zero electrostatic field at a certain point far from the channel, in the GaN buffer, is assumed). The device that we are considering is a normally on FET, and to determine the charge in the channel and the bandstructure at zero volts we have to solve the self-consistent problem. When the reverse bias applied to the gate increases, the charge in the channel decreases, and eventually disappears at a voltage called the threshold voltage V_{th}. For even higher reverse biases, a depletion region in the buffer is formed, associated with the residual donors in the GaN layer, and whose width increases for more negative gate voltages. For reverse voltages greater or equal to V_{th}, the electrostatic

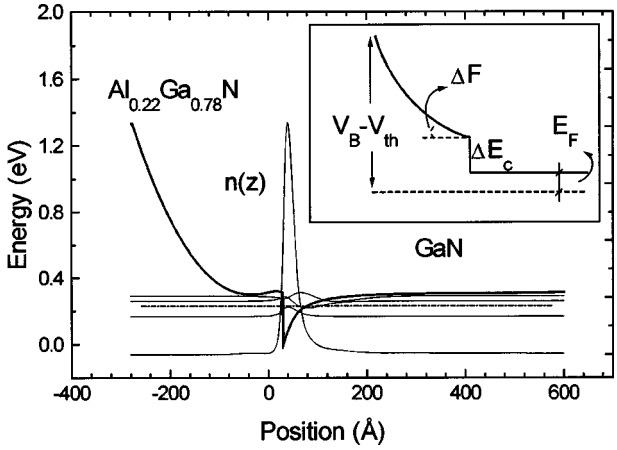

FIG. 4. Calculated conduction-band profile at 0 V for the HFET structure described in the text. The corresponding low-energy wave functions and charge distribution are also shown. The Fermi level is plotted with dot-dashed line. The sketch of the potential profile in the case of depleted channel is included in the inset, with the definition of different symbols used in the text.

problem is similar to the one solved for the multiple quantum well structure, but having only one $Al_xGa_{1-x}N$/GaN heterojunction and a varying doping distribution. To estimate V_{th} we can use an expression similar to Eq. (15), making zero the field due to the confined charge, and including the applied bias at threshold, the Schottky barrier height V_B, the conduction-band discontinuity ΔE_c, and the position of the Fermi level with respect to the GaN conduction band E_F. We can write that

$$(-V_{th}+V_B-\Delta E_c+E_F)=\Delta F L_b+\frac{qN_dW^2}{2\kappa}, \qquad (17)$$

where L_b is the total thickness of the $Al_xGa_{1-x}N$ (spacer and doped barrier) and W is the thickness of the doped region. The conduction-band profile corresponding to this depletion situation is shown in the inset to Fig. 4.

For voltages of magnitude lower than the threshold voltage, the confined charge determines the band structure and vice versa; we have used the self-consistent model to calculate the charge in the channel and compared the result with that determined from capacitance-voltage measurements at zero volts applied to the gate. The results of this calculation are plotted in Fig. 4. By using the theoretical value of the polarization fields,[9] the calculated charge in the channel is $1.1\times10^{13}\,cm^{-2}$, whereas the measured value is $6.4\times10^{12}\,cm^{-2}$. The origin of this discrepancy could, in principle, be related to the uncertainties in the structural parameters used in the simulation: Al composition, thicknesses, Schottky barrier height, background doping, and intentional doping concentration, among others. Therefore, it has been necessary to analyze the structure by using several physical characterization techniques, to reduce the number of variables, as described in Ref. 4. The Al composition, thicknesses, and intentional doping given above are the result of such analysis. A Schottky barrier height of 1.44 V and background doping of $10^{17}\,cm^{-3}$ are assumed. Thus, we determined a polarization field (field discontinuity ΔF) that simultaneously fits the experimental values of both the

threshold voltage and the charge in the channel with zero volts applied. Expression (17) and self-consistent simulations were used, respectively. For an Al content of 0.22, we have found a polarization field of 1.2 MV/cm, as compared to the 2.3 MV/cm theoretically determined.[9] As in the MQW case analyzed in the previous section, it cannot be said, from this study, whether the spontaneous polarizations or piezoelectric constants are wrong or there is a source of extra polarization at the GaN/$Al_xGa_{1-x}N$ interfaces. The situation is similar to the one found in piezoelectric [111]-oriented $In_xGa_{1-x}As$ quantum wells, where the initially predicted reduction in the piezoelectric constants is still under discussion.[19,20]

V. CONCLUSIONS

We have shown how the device structure determines the internal distribution of electric fields in GaN-based heterostructures. Basic undoped structures and doped heterojunctions have been analyzed. Doping distributions, compositions and thicknesses of the layers, and the boundary conditions have to be taken into account for a proper description of the bandstructure. Analytical expressions for the electric fields have been obtained, the cases where they can be used have been discussed, and they are intended to help in the design of heterojunction structures when a tailoring of the electric field is required. Self-consistent calculations are needed to describe the potential variations when there is charge accumulation at the interfaces. This may be the case even in nominally undoped $Al_xGa_{1-x}N$/GaN MQW structures, as it has been analyzed here. In MQW structures and in HFET devices, by comparing our calculations with experimental results, polarization-induced field discontinuity significantly lower (down to 50%) than the values deduced from the theoretical spontaneous and piezoelectric polarizations have been obtained for $Al_xGa_{1-x}N$ layers with Al contents of 11% and 22%.

ACKNOWLEDGMENTS

The authors would like to thank Dr. M. Leroux for helpful discussions and sample data information in relation to the results reported in Ref. 8. The financial support from CICYT Project No. MAT98-0823-C03-01 is acknowledged.

[1] S. Nakamura and G. Fasol, *The Blue Laser Diode* (Springer-Verlag, Berlin, 1997).
[2] M. S. Shur, Solid-State Electron. **42**, 2131 (1998).
[3] O. Ambacher, J. Smart, J. R. Shealy, N. G. Weimann, K. Chu, M. Murphy, W. J. Schaff, L. F. Eastman, R. Dimitrov, L. Wittmer, M. Stutzmann, W. Rieger, and J. Hilsenbeck, J. Appl. Phys. **85**, 3222 (1999).
[4] J. A. Garrido, J. L. Sánchez-Rojas, A. Jimenez, E. Muñoz, F. Omnes, and P. Gibart, Appl. Phys. Lett. **75**, 2407 (1999).
[5] T. Takeuchi, C. Wetzel, S. Yamaguchi, H. Sakai, H. Amano, I. Akasaki, Y. Kaneko, S. Nakagawa, Y. Yamaoka, and N. Yamada, Appl. Phys. Lett. **73**, 1691 (1998).
[6] J. S. Im, H. Kollmer, J. Off, A. Sohmer, F. Scholz, and A. Hangleiter, Phys. Rev. B **57**, R9435 (1998).
[7] H. S. Kim, J. Y. Lin, H. X. Jiang, W. W. Chow, A. Botchkarev, and H. Morkoc, Appl. Phys. Lett. **73**, 3426 (1998).
[8] M. Leroux, N. Grandjean, M. Laügt, J. Massies, B. Gil, P. Lefebvre, and P. Bigenwald, Phys. Rev. B **58**, R13 371 (1998).
[9] F. Bernardini, V. Fiorentini, and D. Vanderbilt, Phys. Rev. B **56**, 10 024 (1997).
[10] A. Hangleiter, J. S. Im, H. Kollmer, S. Heppel, J. Off and F. Scholz, MRS Internet J. Nitride Semicond. Res. **3**, 15 (1998).
[11] F. Bernardini and V. Fiorentini, Phys. Rev. B **57**, R9427 (1998).
[12] A. D. Bykhovski, B. L. Gelmont, and M. S. Shur, J. Appl. Phys. **81**, 6332 (1997).
[13] D. L. Smith and C. Mailhiot, Phys. Rev. Lett. **58**, 1264 (1987).
[14] B. K. Laurich, K. Elcess, C. G. Fonstad, J. G. Beery, C. Mailhiot, and D. L. Smith, Phys. Rev. Lett. **62**, 649 (1989).
[15] J. L. Sánchez-Rojas, A. Sacedón, F. Calle, E. Calleja, and E. Muñoz, Appl. Phys. Lett. **65**, 2214 (1994).
[16] S. M. Sze, *Physics of Semiconductor Devices* (Wiley-Interscience, New York, 1981).
[17] J. L. Sánchez-Rojas and E. Muñoz, in *Proceedings of the IEEE/Cornell Conference on Advanced Concepts in High Speed Semiconductor Devices and Circuits*, 1993, p. 431.
[18] H. Shen and M. Dutta, J. Appl. Phys. **78**, 2151 (1995).
[19] J. L. Sánchez-Rojas, A. Sacedón, F. Gonzalez-Sanz, E. Calleja, and E. Muñoz, Appl. Phys. Lett. **65**, 2042 (1994).
[20] P. Ballet, P. Disseix, J. Leymarie, A. Vasson A-M. Vasson, and R. Grey, Phys. Rev. B **59**, R5308 (1999).